

Nucleation of Fe nanoparticle chains and nanostructures on Au(111) stepped surface

Wen-Chin Lin,¹ Hung-Yu Chang,² Yen-Yin Lin,¹ Yu-Cheng Hu,² Chuang-Han Hsu,¹ and Chien-Cheng Kuo^{2,3,a)}

¹Department of Physics, National Taiwan Normal University, 11677 Taipei, Taiwan

²Department of Physics, National Sun Yat-sen University, 80424 Kaohsiung, Taiwan

³Center for Nanoscience and Nanotechnology, National Sun Yat-sen University, 80424 Kaohsiung, Taiwan

(Received 5 November 2009; accepted 24 November 2009; published online 4 January 2010)

Nucleation of regular nanoparticle chains, Fe nanostructures, and nanoisland array was demonstrated on Au(111) stepped surface, by different growth methods. With Xe buffer layer assisted growth, nanoparticles segregated right at the descending step edges, forming nanoparticle chains. Two-step growth (200 K deposition+300 K annealing) of Fe on properly chosen step (width = 4.3 ± 0.2 nm) resulted in single atomic height nanostructures at the descending edges. Through the multistep growth, $3 \times (0.15 \text{ ML Fe}/8 \text{ L Xe at } 90 \text{ K} + 350 \text{ K annealing})$ on 0.05 ML seeds, a regular bilayer-island array was prepared. The detailed nucleation mechanism is discussed. Our experimental observation manifests the possibilities for the preparation of various one-dimensional nanostructures on Au(111) stepped surface. It is especially important for future studies and applications in nanoscale magnetism and catalysis. © 2010 American Institute of Physics. [doi:10.1063/1.3275419]

I. INTRODUCTION

Due to the symmetry breaking, characteristic physical properties are expected in low-dimensional systems.¹⁻⁷ In particular, one-dimensional (1D) magnetic materials attract much theoretical and experimental efforts, in the crucial fabrication methods and in the complex of magnetic behavior.^{2,3} In 1D magnetic systems, because of the high ratios of surface/volume atom and length/width, surface and shape anisotropy are significant and usually in competition with each other.⁴⁻⁷ Thus, one can expect to change the magnetic behavior of 1D nanostructures through the modulation of spacial arrangement, shape, or density. However, in reality the manipulation is still challenging. So far, stepped surfaces are frequently used for self-organized 1D systems in ultrahigh vacuum condition. About 50 years ago, the ascending edges of the stepped surface have been proposed to be 1D trapping lines for deposit atoms.^{8,9} The idea has been proved and applied in many different combinations of deposit and substrate, for example, Fe,Cu/W(110).^{5,10} In the report of Gambardella *et al.*,^{11,12} the Co monatomic chains were successfully prepared on Pt(997) stepped surface, triggering the sequential studies of 1D magnetic material on similar stepped surfaces. In our study, the following nucleation mechanisms were demonstrated to generate various Fe nanostructures on Au(111) stepped surface.

The first idea is “buffer layer assisted growth (BLAG) on stepped surface.” BLAG has been extensively used for fabrication of three-dimensional (3D) nanoparticle assemblies with controlled sizes for a wide variety of materials and substrate.¹³⁻¹⁵ Kerner and Asscher¹⁶ reported the buffer layer assisted laser patterning of Au nanoparticle stripes on

Ru(001). Antonov *et al.*¹⁷ reported on the preparation of CdSe quantum dots and rods by BLAG, with characteristic photoluminescence.

Concerning the magnetic properties, due to the limitation of self-organization, 1D atomic chains or nanostructures are usually too thin or too small, leading to the very low Curie temperature, which cannot fit the room temperature applications.¹⁸ BLAG is a feasible method for fabrication of nanoparticles with larger diameter and desired aspect ratios. The problem of low Curie temperature could be overcome in this way. Thus, the idea proposed in this paper is performing BLAG on stepped surface. The formation of 1D nanoparticle chains are expected.

The second idea is “two-step growth,” combining low-temperature growth and postannealing. In contrast to the conventional nucleation at ascending edges, Fe/Cu(111) vicinal surface was shown to be a very special case, revealing self-assembled nanostructures at descending edges.^{6,19} The unique nucleation mechanism attracted much attention. The subsequent theoretical simulations and experiment were launched for the detailed understanding.^{20,21} Our study of Fe nanostructures/Au(111) steps also reveals the unconventional nucleation at descending edges. The possible mechanism will be discussed in the text.

Besides of the conventional nanostructures or atomic chains decorated at step edges, Au(788) has been shown to be a good template for self-organized Co and Fe nanodot arrays, by combing the surface steps and surface reconstruction.^{22,23} Our study revealed that the introduction of a few Xe buffer layer significantly change the morphology into a complex array of biatomic and monatomic height islands. The above proposed ideas were clearly demonstrated in this report. These methods, especially the third one, can be extended in

^{a)}Author to whom correspondence should be addressed. Electronic mail: cckuo@faculty.nsysu.edu.tw.

wide range of deposit and substrate materials. The grown patterns are also of full interests for further magnetic measurements and theoretical simulations.

II. EXPERIMENT

The experiments were performed in multifunctional ultrahigh vacuum (UHV) chambers with the base pressure lower than 4×10^{-11} mbar. The sample preparation and characterization were *in situ* carried out. After cycles of 500 eV Ar^+ sputtering and annealing, clean and well-ordered Au(111) surface was prepared. We focused on the surface areas with high density of naturally formed atomic steps. Fe atoms evaporated by e-beam heating were deposited while the substrate temperature is at 33–200 K, depending on which growth method was adopted. The deposition rate of Fe nanostructures was 3×10^{-3} ML/s. For Fe island array and nanoparticles, the deposition rate was $(6-9) \times 10^{-4}$ ML/s. The adsorption of Xe, and subsequently deposition of Fe were performed at 90 or 33 K. Then, the sample was annealed to 300 K for the desorption of Xe and formation of Fe nanostructures. The Fe nucleation behavior was investigated by UHV-scanning tunneling microscopes (STM).

III. RESULTS AND DISCUSSION

A. BLAG: Nanoparticle chains

BLAG has been shown to be a feasible method for fabrication of 3D nanoparticle assemblies on various surfaces.¹³⁻¹⁸ However, the control and patterning of nucleation position is still crucial and recently attracts much attention.¹³⁻¹⁷ In our experiment, the combination of BLAG on stepped surface is demonstrated to be a good method to trap the nanoparticles at the step edges and assemble them into nanoparticle chains. Figure 1(a) shows the growth results of 0.6 ML Fe on Au(111) herringbone surface by 8 L Xe-BLAG at 33 K with subsequent 300 K annealing. On the terrace, the nanoparticles distribute randomly and the herringbone pattern is irrelevant to the particle position. In the magnified images of Figs. 1(b) and 1(c), one can observe that the Fe nanoparticles nucleate at the step edges. From the line profile shown in Fig. 1(d), the nanoparticles reach multi-atomic height, upto ~ 1 nm, which is much larger than the conventional single-atomic height islands by direct deposition.²⁴ Figure 1(e) exhibits the line profiles across the steps. From the comparison between line profiles, one can clearly observe that Fe nanoparticles nucleate at the descending edges.

Concerning the Fe nanoparticle size, Fig. 2 summarized the statistics of particle height and diameter. The size distribution of nanoparticles on terrace and step edges are denoted with different notations, for comparison. It can be clearly concluded that the nanoparticles nucleated on terrace (diameter = 5.4 ± 0.4 nm, height = 1 ± 0.5 nm) are apparently larger than those on step edges (diameter = 4 ± 0.2 nm, height = 0.6 ± 0.4 nm). In detailed examination, most of the large step particles are contributed from the first descending edge. These observations are close to the intuitive expectation since the extensive terrace can aggregate more Fe atoms, forming larger nanoparticles.

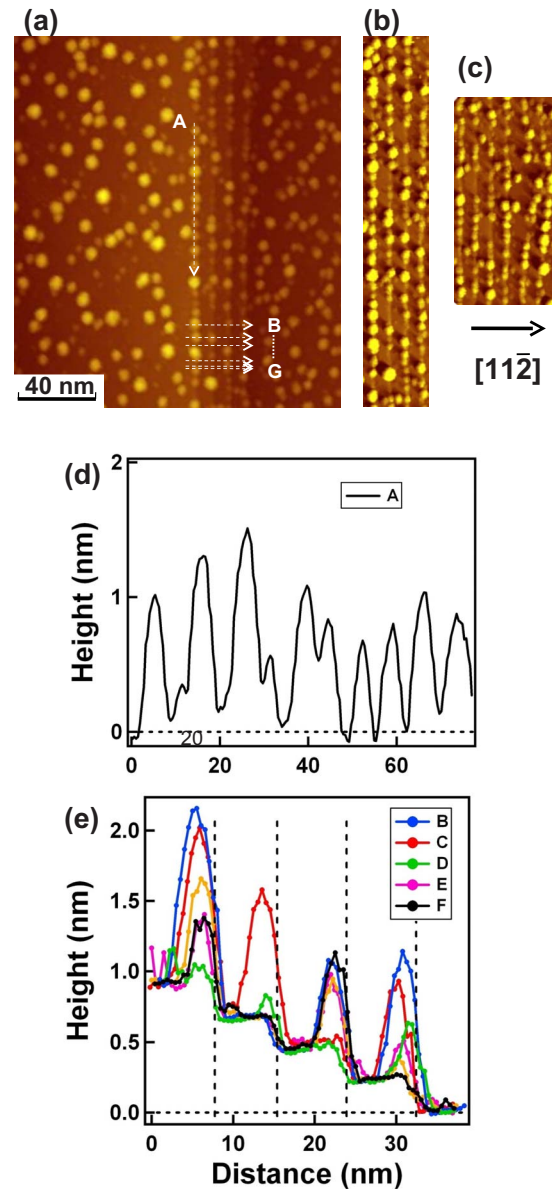


FIG. 1. (Color online) STM images of 0.6 ML Fe on Au(111) surface by 8 L Xe BLAG at 33 K with subsequent 300 K annealing. For comparison, (a) reveals the growth result on surface combing terraces and steps. (b) and (c) are magnified images at steps. (d) and (e) exhibit line profiles along and across the steps, as indicated in (a). The cross sections indicates clearly the nanoparticles nucleate at the descending edges.

It was known that the particle size can be controlled through the thickness of Xe buffer layer, as well as the deposit coverage.¹³⁻¹⁵ However, the effect of surface (template) morphology is seldom mentioned. In a simplified picture of BLAG, first, nanoparticles are gradually formed by aggregating more and more deposit atoms during the Xe desorption. That is why more deposit atoms and thicker Xe buffer layer can result in larger particle size. Second, when close to the end of Xe desorption, the residual Xe atoms on the surface might promote the surface diffusion of small nanoparticles, constructing large ones. Besides, the dewetting-driven model has been performed by Palmer *et al.*,²⁵ suggesting that the microstructure of the substrate plays a role in the BLAG process. Concerning the dewetting of Xe layers and surface diffusion, it is straight forward to expect that the surface

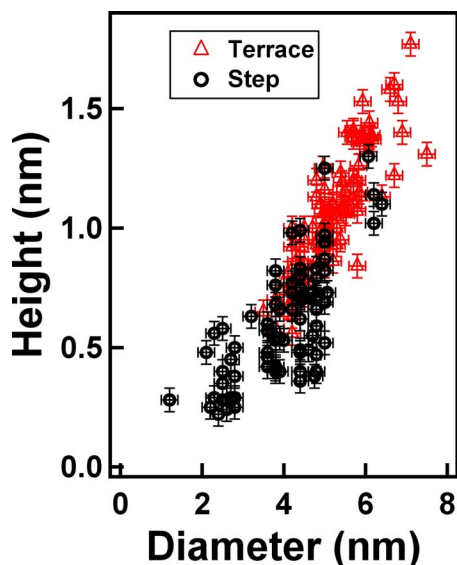


FIG. 2. (Color online) Height-diameter plot of Fe nanoparticles on the terraces and the steps, respectively, for comparison.

morphology will significantly change the result of BLAG. Steps on a surface may act as nucleation sites for dewetting, leading to cluster decoration of steps. Actually, Zhang *et al.*²⁶ showed that Fe clusters were aligned into linear chains on Pt(997) by BLAG. Our growth result of Fe nanoparticle chains on Au(111) stepped surface clear reveals that the preferred nucleation sites are the descending edges. The statistics shown in Fig. 2 indicates the critical role played by surface morphology: terraces or steps. Not only soft landing but also Xe dewetting, surface diffusion and aggregation are important. The later mechanism, in particular, provides us the possibility to arrange the nanoparticles into regular patterns. Besides, one interesting question could be asked: does the step effect work with high coverage of Xe buffer layer? In the method of BLAG, no matter how thick the original Xe buffer layer is, the Xe coverage will gradually decrease during the processes of Xe-desorption/Fe nanoparticle landing, until no Xe on the surface. While close to the end of the Xe-desorption/Fe nanoparticle landing processes, the residual Xe buffer layer will be very thin and the attraction of surface steps might still function. Since our experimental data is limited to only low coverage of Xe, we cannot claim that the surface steps will always attract nanoparticles, even with high coverage of Xe. The validity of discussion should be limited to current low thickness of Xe buffer layer. The further experiments with high coverage of Xe buffer layer are worthy to study, in order to clarify the above discussion.

B. Two-step growth: Nanostripes

Two-step growth is performed by Fe deposition at 200 K with subsequent 300 K annealing. The combination of low-temperature deposition and postannealing has been frequently used in preparation of quantum well thin film systems²⁷ because low-temperature-growth can reduce interdiffusion at the interface, and thermal annealing at suitable temperature may smoothen the surface roughness. In the studies of Rohart *et al.*,²³ while 0.35 ML Fe was deposited

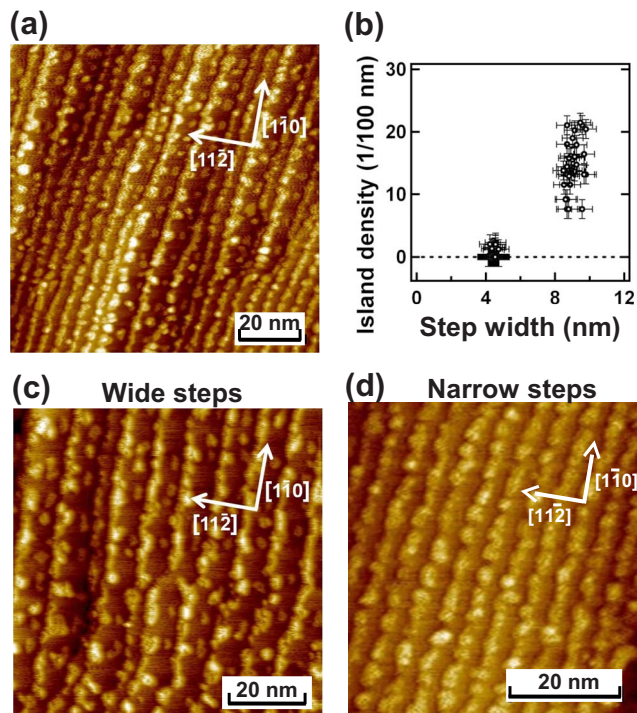


FIG. 3. (Color online) (a) STM image of 0.35 ML Fe deposited on Au(111) stepped surface at 200 K with subsequent 300 K annealing (two-step growth). (b) is the statistics of island density (number/100 nm step length), as a function of step width, indicating two preferred step widths, i.e., 4.3 ± 0.2 nm and 8.5 ± 0.4 nm. [(c) and (d)] STM images of 0.35 ML Fe nanostructures grown on wide and narrow steps, respectively.

onto Au(788) stepped surface at 165–200 K. Regular Fe dot arrays could be observed at the deposition temperature, without annealing. For 250 K deposition, the beginning of step-flow growth started to be seen. 200 K was shown to be a crucial temperature related to the transition of growth mode and thus was chosen here to perform the two-step growth.

The morphology of 0.35 ML Fe/Au(111) stepped surface, grown by two-step method, is shown in Fig. 3. Figure 3(a) reveal the large scale image. The statistics of isolated island density (number per 100 nm step length) is summarized in Fig. 3(b). There are two kinds of naturally preferred step widths, 4.3 ± 0.2 and 8.5 ± 0.4 nm. On the narrow steps [Fig. 3(d)], only single atomic height nanostripes nucleates at the descending edges. On the wide steps [Fig. 3(c)], not only nanostripes, but also isolated islands on the step terrace can be observed. Steps with larger width allow the formation of 10–20 isolated islands per 100 nm step length. It might be correlated with the herringbone structure on Au(111) terrace. The size of the herringbone structure unit is $7.2 \times 8\text{--}50$ nm.^{24,28} The periodicity along $[1\bar{1}0]$ ranges 8–50 nm, depending on the preparation processes and defect density. The periodicity along $[11\bar{2}]$ always sticks to 7.2 nm.²⁸ Therefore, for step width larger than 7.2 nm, it is possible to form the next herringbone kinks, which are preferred nucleation sites for single layer islands. For the narrower steps, the condition is similar to the previously reported Au(778) surface, in which a periodic reconstructed structure is formed along the step edges.²³ The terraces are constituted of regular fcc and hcp areas. Actually, in more detailed examination of

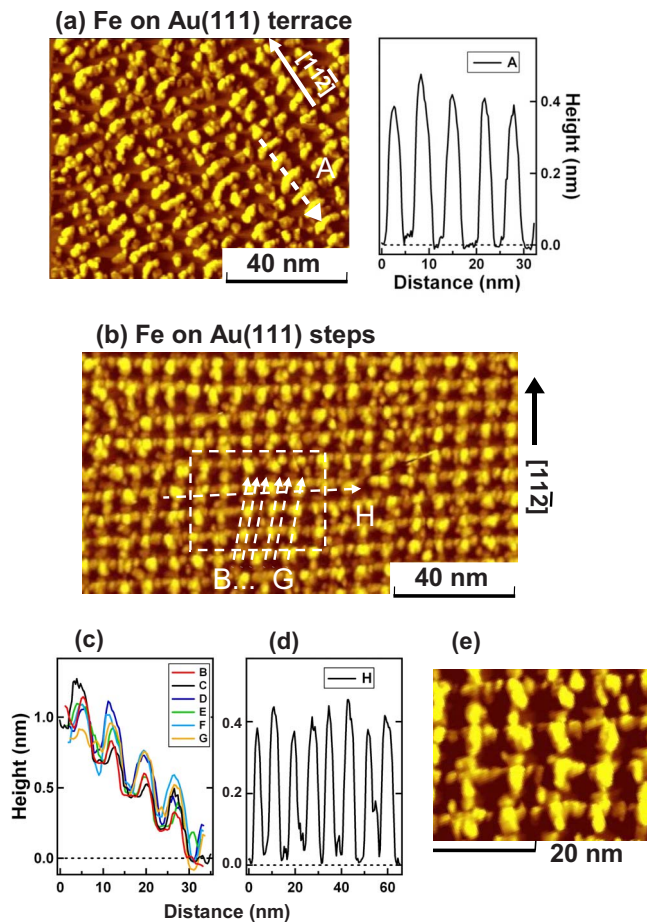


FIG. 4. (Color online) STM images of Fe on Au(111) surface by multistep growth method, $3 \times (0.15 \text{ ML Fe}/8 \text{ L Xe exposure at } 90 \text{ K} + 350 \text{ K annealing})$ on 0.05 ML seeds. (a) The growth result on terrace. The section line profile indicates the regular biatomic height elongated islands. (b) The growth result on regular steps. [(c) and (d)] The line profiles along and across the steps. (e) Magnified STM image, as indicated in (b).

Fig. 3, the nanostripes decorated on step edges seems formed by connections between nearby islands. By 200 K deposition, the Fe dots might first nucleates at the preferred periodic fcc regions, and then be connected by sequential deposition or 300 K annealing.²³ The detailed theoretical simulation and characterization are apparently beyond the scope of this paper, but can be interesting for the future study.

C. Multistep growth: Island array

Besides of the above 200 K growth, Xe buffer layer is used to modulate the nucleation and mobility of deposit. 8 L Xe adsorption and subsequent Fe deposition is performed at 90 K, on top of the predeposited 0.05 ML Fe nucleation seeds. Usually, thick Xe buffer layers adsorb at 50 K, and turn the growth mode into nanoparticle assemblies. Most of Xe desorb before 90 K. Nevertheless, in our previous studies, even the residual submonolayer Xe at 90 K can change the Fe nucleation behavior seriously.²⁴

For comparison, Fig. 4(a) reveals the multistep growth, $3 \times (0.15 \text{ ML Fe}/8 \text{ L Xe at } 90 \text{ K} + 350 \text{ K annealing})$ on 0.05 ML seeds/Au(111) terrace.²⁴ The surface is composed of regular biatomic height Fe islands with an elongated

shape. There are small single-atomic height islands distributing between the elongated ones. This multistep growth actually brings about the complex Fe island array, which is totally different from the conventional single-atomic height island assemblies by RT-deposition.^{24,29,30}

The growth results on Au(111) stepped surface are shown in Figs. 4(b)–4(e). From the line profiles in Fig. 4(c), the island nucleation at atomic steps can be recognized. The line profile in Fig. 4(d) indicates the biatomic height islands. The magnified image, shown in Fig. 4(e), clearly exhibits the details. The biatomic height islands nucleate at the descending edges with regular periodicity. Particularly, there are small single-atomic height islands bridging the nearby biatomic height islands. With the regular steps width, one can fabricated the well-ordered network consisted of regular single and biatomic height islands.

In comparison with the conventional direct deposition, the residual Xe adsorbed at 90 K indeed affects the nucleation and surface diffusion mechanism seriously, leading to the bilayer islands. After combing the 350 K thermal annealing, multistep growth results in not only more 3D, but also regular Fe islands array.

IV. SUMMARY

Fabrication of regular Fe nanoparticle chains, nanostripes, and island arrays was demonstrated on Au(111) stepped surface, by various growth methods. These nucleation behaviors are distinct from conventional results of direct deposition. The nucleation mechanisms of regular biatomic height island arrays and BLAG on steps are worth further theoretical simulation. These demonstrated growth results will be valuable in the future studies and applications in magnetism. The complex interrelation between 1D geometry, structural transition, and magnetic behaviors will be very interesting to explore.

ACKNOWLEDGMENTS

This work was supported by the National Science Council of Taiwan under Grant Nos. NSC 96-2112-M-003-015-MY3, NSC 96-2112-M-110-002, and NSC 97-2112-M-110-003-MY3.

¹D. Sánchez-Portal, S. Riikonen, and R. M. Martin, *Phys. Rev. Lett.* **93**, 146803 (2004).

²F. J. Himpsel, J. E. Ortega, G. J. Mankey, and R. F. Willis, *Adv. Phys.* **47**, 511 (1998).

³J. Shen and J. Kirschner, *Surf. Sci.* **500**, 300 (2002).

⁴J. P. Pierce, M. A. Torija, Z. Gai, J. Shi, T. C. Schultess, G. A. Farnan, J. F. Wendelken, E. W. Plummer, and J. Shen, *Phys. Rev. Lett.* **92**, 237201 (2004).

⁵H. J. Elmers, J. Hauschild, H. Hoche, U. Gradmann, H. Bethge, D. Heuer, and U. Kohler, *Phys. Rev. Lett.* **73**, 898 (1994).

⁶J. Shen, R. Skomski, M. Klaua, H. Jenniches, S. S. Manoharan, and J. Kirschner, *Phys. Rev. B* **56**, 2340 (1997).

⁷S. Shiraki, H. Fujisawa, T. Nakamura, T. Muro, M. Nantoh, and M. Kawai, *Phys. Rev. B* **78**, 115428 (2008).

⁸G. A. Bassett, *Philos. Mag.* **3**, 1042 (1958).

⁹H. Bethge, *Phys. Status Solidi* **2**, 775 (1962); *Surf. Sci.* **3**, 33 (1965).

¹⁰Y. W. Mo and F. J. Himpsel, *Phys. Rev. B* **50**, 7868 (1994).

¹¹P. Gambardella, M. Blanc, L. Burgi, K. Kuhnke, and K. Kern, *Surf. Sci.* **449**, 93 (2000).

¹²P. Gambardella, A. Dallmeyer, K. Maiti, M. C. Malagoli, W. Eberhardt, K.

- Kern, and C. Carbone, *Nature (London)* **416**, 301 (2002).
- ¹³L. Huang, S. Jay Chey, and J. H. Weaver, *Phys. Rev. Lett.* **80**, 4095 (1998).
- ¹⁴G. D. Waddill, I. M. Vitomirov, C. M. Aldao, S. G. Anderson, C. Capasso, J. H. Weaver, and Z. Liliental-Weber, *Phys. Rev. B* **41**, 5293 (1990).
- ¹⁵C. Haley and J. H. Weaver, *Surf. Sci.* **518**, 243 (2002).
- ¹⁶G. Kerner and M. Asscher, *Nano Lett.* **4**, 1433 (2004).
- ¹⁷V. N. Antonov, P. Swaminathan, J. A. N. T. Soares, J. S. Palmer, and J. H. Weaver, *Appl. Phys. Lett.* **88**, 121906 (2006).
- ¹⁸O. Fruchart, M. Eleoui, J. Vogel, P. O. Jubert, A. Locatelli, and A. Ball-estrazzi, *Appl. Phys. Lett.* **84**, 1335 (2004).
- ¹⁹A. Brodde, K. Dreps, J. Binder, Ch. Lunau, and H. Neddermeyer, *Phys. Rev. B* **47**, 6609 (1993).
- ²⁰N. N. Negulyaev, V. S. Stepanyuk, W. Hergert, P. Bruno, and J. Kirschner, *Phys. Rev. B* **77**, 085430 (2008).
- ²¹J. Guo, Y. Mo, E. Kaxiras, Z. Zhang, and H. H. Weitering, *Phys. Rev. B* **73**, 193405 (2006).
- ²²N. Weiss, T. Cren, M. Epple, S. Rusponi, G. Baudot, S. Rohart, A. Tejada, V. Repain, S. Rousset, P. Ohresser, F. Scheurer, P. Bencok, and H. Brune, *Phys. Rev. Lett.* **95**, 157204 (2005).
- ²³S. Rohart, Y. Girard, Y. Nahas, V. Repain, G. Rodary, A. Tejada, and S. Rousset, *Surf. Sci.* **602**, 28 (2008).
- ²⁴W. C. Lin, H. Y. Chang, Y. T. Hu, and C. C. Kuo, *Jpn. J. Appl. Phys.* **48**, 08JB07 (2009).
- ²⁵J. S. Palmer, P. Swaminathan, S. Babar, and J. H. Weaver, *Phys. Rev. B* **77**, 195422 (2008).
- ²⁶J. Zhang, D. Repetto, V. Sessi, J. Honolka, A. Enders, and K. Kern, *Eur. Phys. J. D* **45**, 515 (2007).
- ²⁷H. Liu, Y. F. Zhanga, D. Y. Wanga, M. H. Pana, J. F. Jiaa, and Q. K. Xue, *Surf. Sci.* **571**, 5 (2004).
- ²⁸H. Bulou, F. Scheurer, P. Ohresser, A. Barbier, S. Stanescu, and C. Quiró, *Phys. Rev. B* **69**, 155413 (2004).
- ²⁹W. C. Lin, H. Y. Chang, Y. T. Hu, and C. C. Kuo, *IEEE Trans. Magn.* **45**, 4037 (2009).
- ³⁰W. C. Lin, H. Y. Chang, Y. C. Hu, Y. Y. Lin, C. H. Hsu, and C. C. Kuo, *Nanotechnology* **21**, 015606 (2010).